Journal of Nano- and Electronic Physics
Vol. **7** No 3, 03025(5pp) (2015)

Журнал нано- та електронної фізики
Том **7** № 3, 03025(5cc) (2015)

Photoluminescence of ZnS Luminophore Sonofragmentated in Isopropyl Alcohol Solution

M. Zakirov[1,*], O. Korotchenkov[1], A. Nadtochiy[1], A. Podolyan[1], K. Svezhentsova[2]

[1] *Taras Shevchenko National University of Kyiv, 01601 Kyiv, Ukraine*
[2] *V. Lashkaryov Institute of Semiconductor Physics, NAS of Ukraine, 03028 Kyiv, Ukraine*

(Received 24 February 2015; published online 20 October 2015)

The work describes the preparation of nanosized zinc sulfide phase with ultrasonic fragmentation of polycrystalline basic material. The spectral and kinetic characteristics of the resulting system were studied. The changes of excitation and relaxation channels in the crystals by their sonofragmentation in a polar solvent are shown.

Keywords: Ultrasonic treatment, Luminophore, Zinc Sulfide, Photoluminescence.

PACS numbers: 71.55. Gs, 73.20.Hb

1. INTRODUCTION

The use of ultrasound for the production of nanomaterials allowed to substantially improve access to a wide range of crystalline nano-semiconductors, but the mechanisms of ultrasound action remain largely unclarified [1]. Chemical and physical effects of ultrasound are not the result of its direct interaction with molecules of the environment. However, these effects come from the concomitant acoustic cavitation that is accompanied by the formation, growth and explosive collapse of bubbles in liquid [2]. In homogeneous liquids, bubble cloud collapse conditions an intense local heating that reaches ~ 5000 K, initiation of significant pressures (~ 10^5 kPa) and enormous heating and cooling rates (~ 10^{10} K/s) within individual submicron reactors [3]. In heterogeneous systems, which include solid and liquid phases, effects of ultrasound action are also associated with cavitation. When a cavitation bubble (with a typical diameter of ~ 50 μm at an ultrasound frequency of about 20 kHz) is destroyed near the surface, which is much larger in size, it demonstrates an asymmetric collapse capable to generate high-speed jets of liquid. At that, velocity of the jets hitting the surface can exceed 100 m/s [4]. The action of these jets can cause local erosion of the surface, its ultrasonic cleaning, activation of chemical transformations near the surface, grinding of solid matter (sonofragmentation) [1]. Cavitation collapse also causes shock waves with a velocity up to 4000 m/s and pressure with an amplitude of ~ 10^6 kPa, which establish the conditions for the occurrence of plastic deformation of various solids and provide high rates of collisions between solid particles of the micron size [5].

Our previous studies of the surface photovoltage in silicon plates immersed in water indicate a substantial influence of ultrasound on the charge transfer at the surface [6]. One observes a significant reduction of the photovoltage decay curve explained by the appearance of dangling bonds on the surface, when the oxide layer is removed by cavitation bubbles in water.

This work is devoted to the experimental study of the features of photoluminescence of ZnS luminophore sonofragmentated in isopropyl alcohol solution. The results obtained provide for the possibility of an effective modification of the charge transfer processes by ultrasound when a semiconductor is placed in a chemically active medium that is important for the practical application of semiconductor structures of the ZnS/ZnO type. Some works indicate the changes in the spectral characteristics depending on the medium, in which a semiconductor structure is placed [7]. Nevertheless, the question about the influence of the medium on the kinetic luminescence characteristics, in particular, for low-dimensional structures, when contribution of the surface, which is in a direct contact with the medium, has the dominant character, remains open.

2. EXPERIMENTAL

ZnS samples were synthesized by the chemical transport method in a closed iodide system. Ampoules were produced of fused quartz glass S5-1 of optical quality. At first, the ampoules were washed 3 times by hot water (at 75 °C), and then 5 times more by distilled water. After that, they were dried for two days in the thermostat at the temperature of 120-150 °C. The sealed ampoules were placed in a two-zone oven, in which the synthesis took place. The synthesis temperature was controlled by chromel-alumel thermocouples.

Zn and S of purity V4 taken in the stoichiometric ratio of m_{Zn} = 6.741 g and m_S = 3.306 g were used for the synthesis. CdI_2 of the mass of 0.2 g was taken as a chemical transport. Evaporation and crystallization temperatures in the oven were, respectively, equal to 1097 °C and 977 °C. Under these conditions, the manufacturing process was kept for 30 hours with subsequent cooling with the rate not more than 10 °C/hour.

The results presented below are obtained for two types of the grown samples designated as samples of type 1 and type 2. The results of X-ray phase analysis indicate that the sample of type 1 contains about 70 % of the sphalerite phase and 30 % of the wurtzite phase, while the sample of type 2 is formed by almost 100 % wurtzite modification.

The synthesized samples showed a quite bright glow at photoexcitation by laser diode with the wavelength of 404 nm (3.07 eV). Photoluminescence (PL) spectra were registered at room temperature using monochromators

* zakyrov@gmail.com

MDR-4 and FEU-79 with computer signal registration. PL kinetics was studied using digital oscilloscope GDS-806S, which provided resolution of 1 μs. PL kinetics was registered during excitation by the same laser diode as during the spectrum recording in the pulse mode with the pulse duration of 50 μs. It is also established in separate experiments that dependence of the PL intensity on the intensity of excitation luminous flux is described by the linear function.

The photovoltage kinetics was registered by the automated installation with contactless method of signal release described in detail in the work [8].

IR studies were performed by the spectrometer Spectrum BX-II FTIR PerkinElmer Inc in the wavenumber range of 500-4000 cm^{-1} at room temperature.

The optical microscope Olympus GX-51 was used in order to estimate the sizes of fragmented particles. Nanosized phase of the samples was investigated by the atomic-force microscopy method on the scanning probe microscope FemtoScan Online. Scanning was carried out in the contact mode in air using cantilevers fpN10S (with radius of curvature of the edge of ≤ 10 nm). Visualization was performed at the temperature of 20-24 °C and air moisture of 50-56 %.

Ultrasound grinding of the grown ZnS samples was performed in a bath with isopropyl alcohol by using the Langevin transducer at a frequency near 30 kHz. Details of the method and installation are given in [6]. For the data presented below, the time of ultrasonic treatment was equal to 5 min. The grinded material was spread in the bulk solution during fragmentation. After termination of the ultrasound action, solution was left for a day for sedimentation of solid particles. At that, the grinded luminophore had a rather wide size spread of fragmented particles. The size of precipitated particles belonged to the micron range. At the same time, nanometer particles, which did not precipitate on the vessel bottom during a week of observations, remained in the solution. Photoluminescence properties of luminophore and FTIR spectra were studied directly in the isopropyl alcohol solution with particles of μm and nm sizes. Kinetics of the photovoltage as well as the microscopic studies were conducted in the same samples obtained during deposition of a drop of liquid with sonofragmented material on a metal (for photovoltage) or mica (for microscopy) surface with subsequent evaporation of alcohol before measurements.

3. RESULTS AND DISCUSSION

The optical and AFM images of the end (a) and the central (b) areas of a dry drop are shown, respectively, in Fig. 1 and Fig. 2. Submicron-size particles, which are not visible in the optical microscope, prevail in the first case, and in the second one – precipitated phase of the sample composed of ZnS particles with sizes to ≈ 200 μm.

The AFM images of the peripheral area of a drop are represented in Fig. 2. It is seen that sizes of sonofragmentated particles in this case are equal to ~ 100 nm. The nanosized and microsized phases of particles were not separated in further studies. At that, the nanosized particles prevail in the sample 1, while in the sample 2 – the micron-size particles.

In Fig. 3 we illustrate the photoluminescence spectra of the samples 1 (a) and 2 (b) before (spectra 1) and after

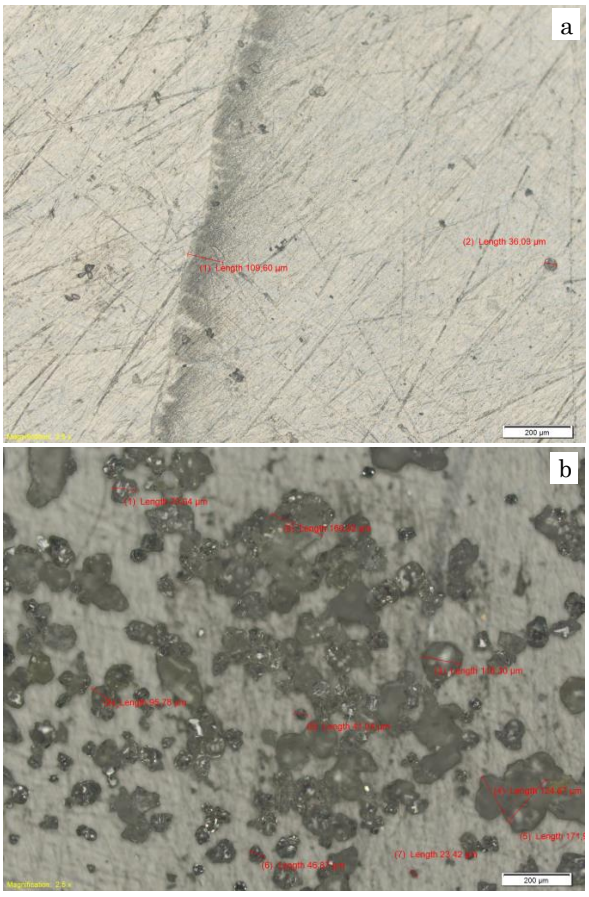

Fig. 1 – Micrographs of the sonofragmentated ZnS luminophore obtained using the optical microscope: (a) – the end area of a dry drop (sample 1); (b) – central area of a drop (sample 2)

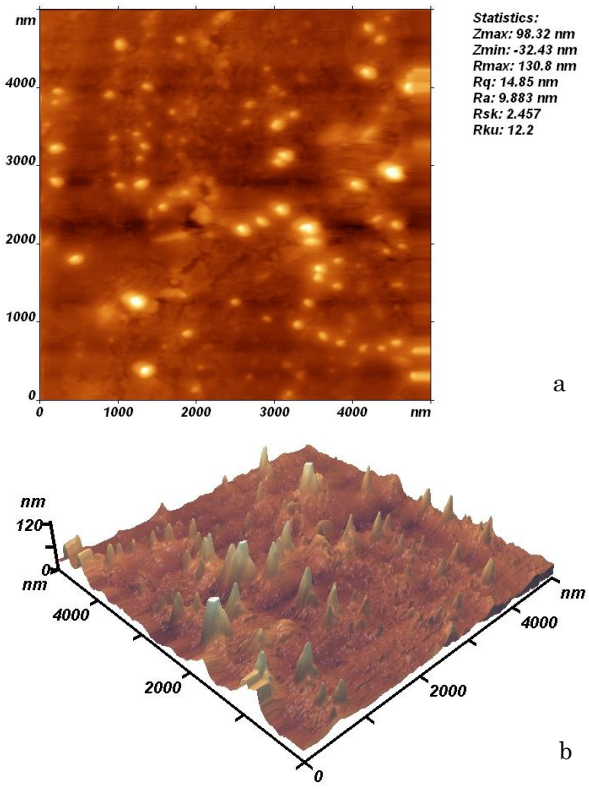

Fig. 2 – AFM-images of the end area of a drop of sonofragmentated ZnS luminophore (sample 1): (a) – 2*D*; (b) – 3*D* images

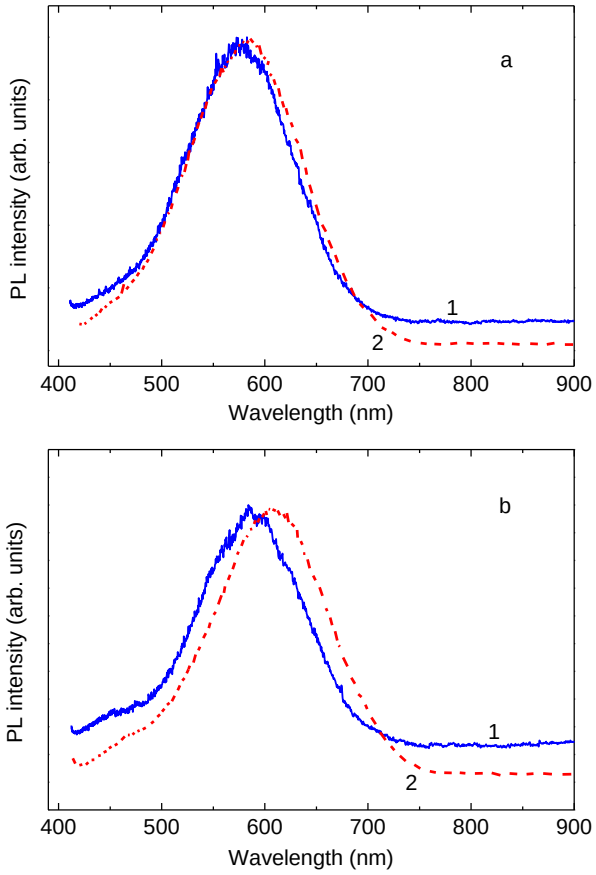

Fig. 3 – Photoluminescence spectra of the samples 1 (a) and 2 (b) before (spectra 1) and after (spectra 2) ultrasonic treatment

(spectra 2) sonofragmentation of limunophore. Sample 1 shows a glow in the band with the maximum at 575 nm (2.16 eV), which is shifted about 10 nm to the longer wavelengths during treatment (to 2.12 eV). Sample of type 2 demonstrates a glow in the band with the maximum at 585 nm (2.12 eV), which is shifted to the longer wavelengths to 610 nm (2.03 eV) during treatment.

It is known that zinc sulfide contains oxygen as a typical impurity. The impact of atmospheric pollutants, ability of ZnS to oxidation and the need to compensate distortions introduced by intrinsic structural defects and impurities favor uncontrolled entry of oxygen into ZnS lattice [9]. An oxide ZnO film is formed on the crystallite surface during surface passivation in the atmosphere.

Based on the literature data, luminescence band with the peak near 610 nm is associated with recombination in ZnS particles performed with the participation of defects [10, 11]. PL band at 575 nm is associated with the negatively charged V_{Zn}^{-} defect, where zinc vacancy acts as the acceptor [12]. The band with the maximum near 585 nm in ZnS structures is associated in literature with the presence of Mn [13].

As known, movement of dislocations from the bulk to the surface and their recapture as well as splitting of particle boundaries formed during the growth are observed under the action of ultrasound in semiconductors of the A^2B^6 compounds [14-16].

We can thus assume that during sonofragmentation a negatively charged zinc vacancy changed its own position and charge due to the exchange of electrons between a dislocation and point defects. The exchange occurred during the movement of a dislocation that caused the shift of the vacancy level to the conduction band bottom.

Kinetics of PL damping registered in the maxima of the radiation bands as well as the kinetics of the photovoltage decay are illustrated, respectively, in Fig. 4 and Fig. 5. Acceleration of the decay kinetics of luminescence and photovoltage after sonofragmentation of luminophore (curves 2 in Fig. 4 and Fig. 5 compared with curves 1) is obvious.

At that, curve 2 in Fig. 5 shows a rapid non-exponential decay within a few milliseconds followed by a sufficiently long exponential relaxation similar, in general, to the photovoltage relaxation in sample 1 (see curve 1 in Fig. 5).

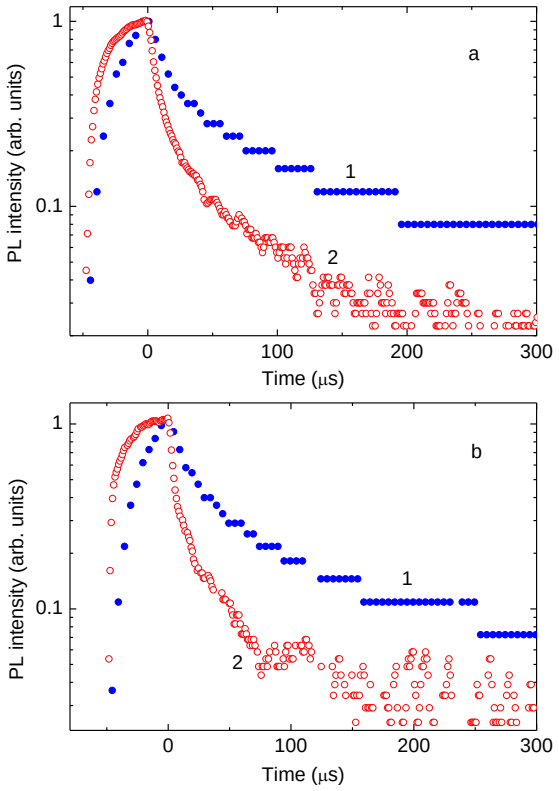

Fig. 4 – PL kinetics of the sample 1 (a) and sample 2 (b) before (curve 1) and after (curve 2) ultrasonic treatment

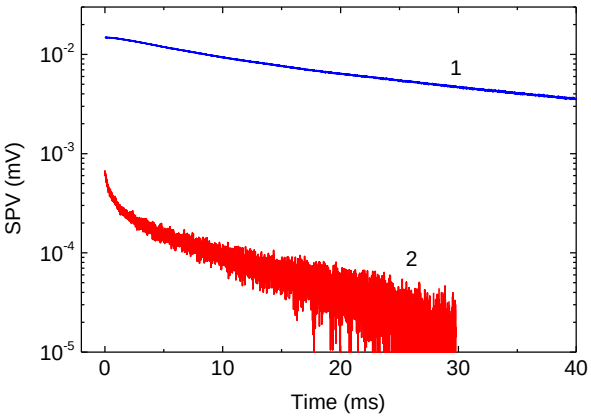

Fig. 5 – Photovoltage kinetics in the sample 1 before (curve 1) and after (curve 2) ultrasonic treatment

The data presented indicate that the dominant excitation and relaxation channels of charge carriers in the samples were changed because of ultrasonic treatment. During sonofragmentation in the liquid medium, the samples are grinded, and their surface is passivated by the chemically active medium. For chemical reasons, it is assumed that OH-groups of isopropyl alcohol are attached to the non-compensated zinc atoms in the near-surface layer (Fig. 6). As a result of this process, a particle of the sample is located in an electric field of alcohol hydroxyl groups attached to it. At that, one can observe a sharp decrease in the value of the photovoltage signal, which in sample 1 is mainly formed in the near-surface region of microcrystallites and is significantly modified in the fragmented sample 2 (surface states N_S and dotted lines of the band bending in the near-surface region of the crystallite in Fig. 6). Passivated bonds, decreasing the photovoltage signal, also ensure a fast recombination channel of photoexcited charge carriers (fast initial decay on the curve 2 in Fig. 5).

Surface modification during sonofragmentation is independently confirmed by the data of infrared absorption illustrated in Fig. 7. They imply that sonofragmentation leads to the shift of the absorption maxima and change in the absorption band intensity of stretching vibrations of the surface hydroxyl groups [18, 19].

Indeed, the band with the peak at 3340 cm^{-1} is associated with vibrations of the OH-group (the shift to 3352 cm^{-1} for sample 1 and 3363 cm^{-1} for sample 2) [20], the band at 2970 cm^{-1} corresponds to asymmetric vibrations in CH_3-sp^3 [21, 22], the bands in the range of 2875-2950 cm^{-1} correspond to vibrations of –C–H [23], the band at 2360 cm^{-1} is associated with adsorption of atmospheric CO_2 on the sample surface [24], the bands at 1115 cm^{-1} and 648 cm^{-1} correspond to the stretching and bending vibrations in the Zn–OH and ZnS systems, respectively [25], the bands at 950 cm^{-1} and 1300-1450 cm^{-1} correspond to C–O stretches on a metal and C–H bends, respectively [26]. Thus, the changes in the peak position and intensity explicitly specify the interaction of the solvent and the studied samples.

The diagram of electronic transitions, which form the PL bands observed, is presented in Fig. 6. Photoexcited electrons are trapped in V_{Zn}^- levels followed by radiation recombination in the PL1 and PL2 transitions for the samples before and after sonofragmentation, respectively. Change in the position of the PL maxima (from PL1 and PL2) can be explained by the change in the energy position of zinc vacancy (solid arrow in Fig. 6).

Thus, it is shown in this work that nanosized phase, which immediately undergoes passivation in the solvent

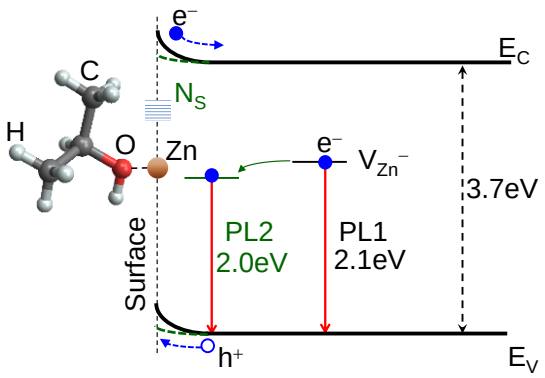

Fig. 6 – Band diagram of ZnS crystallites, which explains the changes in the PL and photovoltage during sonofragmentation. PL1 and PL2 are the electronic transitions, which form the PL spectra before and after sonofragmentation, respectively, e^- and h^+ are the electron and hole, respectively, N_S are the states on the nanocrystallite surface caused by passivation of Zn atoms by OH-groups. Dotted arrows illustrate separation of e^- and h^+ in the near-surface electric field, solid arrow – decrease in the level energy during sonofragmentation. Dotted lines show the decrease in the band bending near the crystallite surface during sonofragmentation

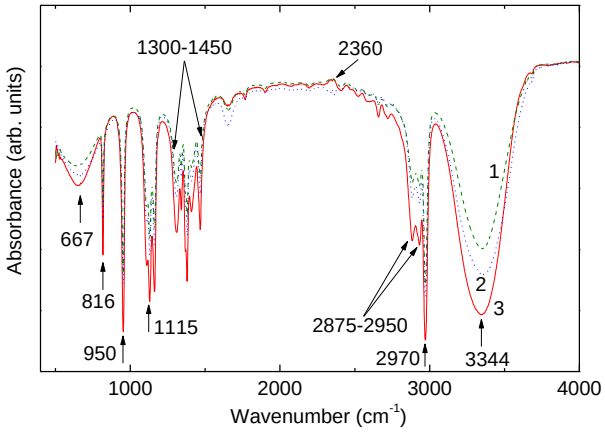

Fig. 7 – FTIR spectra of sample 1 (curve 1), sample 2 (curve 2) and isopropyl alcohol (curve 3) after ultrasonic treatment

medium, is formed in a polar solvent during sonofragmentation of zinc sulfide (both sphalerite and wurtzite). A slight decay of the luminescence yield, change in the excitation and relaxation channels during sonofragmentation is mentioned.

The authors are grateful to the Department of physics of Kamyanets-Podilsky Ivan Ohienko National University for the growth of the initial ZnS crystals.

REFERENCES

1. J.R.G. Sander, B.W. Zeiger, K.S. Suslick, *Ultrasonics Sonochemistry* **21**, 1908 (2014).
2. *Theoretical and Experimental Sonochemistry Involving Inorganic Systems* (Ed. by Pankaj, M. Ashokkumar) (Springer-Verlag: Berlin: 2011).
3. D.J. Flannigan, K.S. Suslick, *Nature* **434**, 52 (2005).
4. J.H. Bang, K.S. Suslick, *Adv. Mater.* **22**, 1039 (2010).
5. R. Pecha, B. Gompf, *Phys. Rev. Lett.* **84**, 1328 (2000).
6. A. Podolian, A. Nadtochiy, V. Kuryliuk, O. Korotchenkov, J. Schmid, M. Drapalik, V. Schlosser, *Sol. Energ. Mater. Sol. C.* **95**, 765 (2011).
7. Yu.Yu. Bacherikov, O.B. Okhrimenko, Z.F. Tomashik, E.M. Lukiyanchuk, K.D. Kardashov, *Zhurn. prikl. spektroskopii* **72**, 799 (2005) [in Russian].
8. A. Podolian, V. Kozachenko, A. Nadtochiy, N. Borovoy, O. Korotchenkov, *J. Appl. Phys.* **107**, 093706 (2010).
9. N.K. Morozova, V.A. Kuznetsov, *Sul'fid tsinka* (M.: Nauka: 1987) [in Russian].
10. D. Kurbatov, A. Opanasyuk, S. Kshnyakina, V. Melnik, V. Nesprava, *Rom. J. Phys.* **55**, 213 (2010).
11. S.I. Bredikhin, S.Z. Shmurak, *JETP* **49**, 520 (1979).
12. K.M. Lee, K.P. O'Donnell, G.D. Watkins, *Sol. State Commun.* **41**, 881 (1982).
13. S. Joicy, R. Saravanan, D. Prabhu, N. Ponpandian, P. Than-

gadurai, *RSC Adv.* **4**, 44592 (2014).
14. Yu.V. Stepanov, V.P. Alekhin, *Fizika i khimiya obrabotki materialov* **1**, 78 (1999) [in Russian].
15. G.Ya. Bazelyuk, I.G. Kozyrskiy, *Fizika metallov i metallovedeniye* **1**, 145 (1971) [in Russian].
16. I.G. Polotskiy, N.S. Mordyuk, *Metallofizika* **29**, 99 (1970) [in Russian].
17. *Basic organic chemistry* (Ed. J.M. Tedder) (London: Wiley: 1966-1975).
18. Yu. Bokker, *Spektroskopiya* (Moskva: Tekhnosfera: 2009) [in Russian].
19. P. Larkin, *Infrared and Raman Spectroscopy; Principle and Spectral Interpretation, 1st Edition* (San Diego: Elsevier: 2011).
20. *Encyclopedia of Nanoscience and Nanotechnology*, (Ed. H.S. Nalwa) **10**, 725 (American Scientific Publishers: 2004).
21. A. Varma, V. Palshin, E.I. Meltis, *Surf. Coat. Tech.* **148**, 305 (2001).
22. Supria N. Rishikeshi, Satyawati Joshi, *J. Therm. Anal. Calorim.* **109**, 1473 (2012).
23. Suprina N. Rishikeshi, Satyawati Joshi, Mayyr K. Temgire, Jayes R. Bellare, *Dalton Trans.* **42**, 5430 (2013).
24. Tabasom Parvin, Namratha Phanichphant, Kullaian Byrappa, *Int. J. Photoenerg.* **2012** ID 670610 (2012).
25. F. Wegmuller, *J. Colloid Interf. Sci.* **116**, 312 (1987).
26. Ravi Shara, *Int. Multidisciplinary Res. J.* 1(9), No8, (2011).